

1 **Causal relationships between gut microbiome, short-chain fatty acids and**
2 **metabolic diseases**

3

4 Serena Sanna ^{1,¶}, Natalie R. van Zuydam ^{2,3,¶}, Anubha Mahajan ^{2,3,¶}, Alexander Kurilshikov ¹,
5 Arnau Vich Vila ^{1,4}, Urmo Võsa ¹, Zlatan Mujagic⁵, Ad A. M. Masclee⁵, Daisy M.A.E.
6 Jonkers⁵, Marije Oosting ⁶, Leo A.B. Joosten⁶, Mihai G. Netea ⁶, Lude Franke ¹, Alexandra
7 Zhernakova ¹, Jingyuan Fu ^{1,7}, Cisca Wijmenga ^{1,8,§}, Mark I. McCarthy ^{2,3,9,§}

8

9 ¹University of Groningen, University Medical Center Groningen, Department of Genetics,
10 Groningen, the Netherlands

11 ²Wellcome Centre for Human Genetics, University of Oxford, Oxford, UK

12 ³Oxford Centre for Diabetes Endocrinology and Metabolism, Churchill Hospital, University
13 of Oxford, Oxford, UK

14 ⁴University of Groningen, University Medical Center Groningen, Department of
15 Gastroenterology and Hepatology, Groningen, the Netherlands

16 ⁵Maastricht University Medical Center, Division Gastroenterology-Hepatology, NUTRIM
17 School for Nutrition, and Translational Research in Metabolism, Maastricht, the Netherlands

18 ⁶Department of Internal Medicine, Radboud Institute of Molecular Life Sciences (RIMLS)
19 and Radboud Center for Infectious Diseases (RCI), Radboud University Medical Center,
20 Nijmegen, the Netherlands

21 ⁷University of Groningen, University Medical Center Groningen, Department of Pediatrics,
22 Groningen, Groningen, the Netherlands

23 ⁸K.G. Jebsen Coeliac Disease Research Centre, Department of Immunology, University of
24 Oslo, Oslo, Norway

25 ⁹Oxford NIHR Biomedical Research Centre, Oxford University Hospitals NHS Foundation
26 Trust, John Radcliffe Hospital, Oxford, UK

27

28 [¶]These authors contributed equally to this work.

29 [§]These authors jointly supervised this work.

30

31 Correspondence should be addressed to S.S. (s.sanna@umcg.nl), C.W.
32 (c.wijmenga@umcg.nl) or M.M. (mark.mccarthy@drl.ox.ac.uk).
33

34 **Microbiome-wide association studies on large population cohorts have highlighted**
35 **associations between the gut microbiome and complex traits, including type 2 diabetes**
36 **(T2D) and obesity¹. However, the causal relationships remain largely unresolved. We**
37 **leveraged information from 952 normo-glycemic individuals for whom genome-wide**
38 **genotyping, gut metagenomic sequence and fecal short chain fatty acid (SCFA) levels**
39 **were available², and combined these with genome-wide association summary statistics**
40 **for 17 metabolic and anthropometric traits. Using bidirectional Mendelian**
41 **Randomization (MR) analyses to assess causality³, we found that host genetic-driven**
42 **increase in gut production of the SCFA butyrate is associated with improved insulin**
43 **response following an oral glucose test ($P = 9.8 \times 10^{-5}$), while abnormalities in**
44 **production or absorption of another SCFA, propionate, are causally related to**
45 **increased risk of T2D ($P = 0.004$). These data provide evidence of a causal effect of the**
46 **gut microbiome on metabolic traits, and support the use of MR as a route to elucidate**
47 **causal relationships from microbiome-wide association findings.**

48 There is increasing evidence that the human gut microbiome plays a role in immune function
49 and metabolic disease^{1,4,5}. Manipulation of the gut microbiome offers an alternative to
50 pharmacological interventions provided it can be demonstrated that altering microbiota
51 composition and/or function (e.g. through personalized nutrition) has clinical benefit. To
52 demonstrate this, it is essential to discriminate between microbiome features that are causal
53 for disease, from those that are a consequence of disease or its treatment, and those that show
54 statistical correlation due to confounding or pleiotropy.

55 Animal studies support a causal role for the gut microbiome in the development of type 2
56 diabetes (T2D), insulin resistance and obesity^{6,7}, but translating these findings to humans and
57 identifying the specific bacterial species responsible has proven challenging⁸. Cross-sectional
58 studies have confirmed that gut microbiota composition is altered in subjects with pre-

59 diabetes or T2D compared to controls, while fecal transplantation studies have shown that
60 insulin sensitivity increases in obese subjects with metabolic syndrome after the transfer of
61 gut microbiota from lean donors^{4,5,9,10}. Whilst the specific microbiome features identified as
62 responsible for these effects have differed between studies, one consistent finding in T2D
63 subjects is a shift in microbiome composition away from species able to produce butyrate.
64 Butyrate and other short-chain fatty acids (SCFAs), such as acetate and propionate, are
65 produced by gut bacterial fermentation of undigested food components. Following absorption
66 by the colonocytes, these SCFAs are either used locally as fuel for colonic mucosal epithelial
67 cells or they enter the portal bloodstream¹¹. While the bulk of evidence suggests that
68 increased SCFA production benefits the host by exerting anti-obesity and anti-diabetic
69 effects^{4,10,12-14}, some *in vitro* and *in vivo* studies have indicated that over-production or
70 accumulation of SCFAs in the bowel may also lead to obesity due to increased energy
71 accumulation^{15,16}. Resolution of these conflicting data requires a detailed understanding of
72 the causal relationships between gut microbiome composition, SCFA abundance and host
73 energy metabolism.

74 Using a Mendelian Randomization (MR) approach³, we set out to identify if any bacterial
75 species or pathways, i.e. sets of species grouped according to the specific functions they play
76 in the gut, have a causal effect on metabolic traits. We and others have recently shown that it
77 is possible to detect variants in the host genome that influence the composition of the gut
78 microbiota^{2,17,18}. This allowed us to deploy a MR approach to infer causal relationships by
79 asking whether genetic predictors of microbiome content influence metabolic traits—or the
80 reverse. This formulation holds even though the quantitative contribution of host genetics to
81 variation in microbiome composition may be limited¹⁹.

82 We assembled genome-wide genetic data, gut metagenomic-sequencing, measurements of
83 fecal SCFAs, and clinical phenotypes for 952 normo-glycemic individuals from the

84 LifeLines-DEEP (LL-DEEP) cohort. From consortium websites (GIANT, MAGIC and
85 DIAGRAM, see URLs), we also gathered publically-available genome-wide association
86 (GWA) summary statistics for 17 anthropometric and glyceic traits²⁰⁻²⁷ (**Supplementary**
87 **Table 1**). We focused our analyses on 245 microbiome features (2 fecal SCFA levels, 57
88 unique taxa, 186 pathways) that were, in LL-DEEP, correlated (false discovery rate (FDR) <
89 0.1) with at least one of the measured anthropometric and metabolic traits (**Methods**,
90 **Supplementary Table 2 and 3**).

91 For each of these features, we sought genetic predictors -- independent genetic variants ($r^2 \leq$
92 0.1), associated ($P < 1 \times 10^{-5}$) with the respective features -- using GWAS data from LL-
93 DEEP, reprocessed from our previous study² (**Methods**). The threshold $P < 1 \times 10^{-5}$ for
94 variant inclusion was identified by maximizing the amount of genetic variance explained by
95 the genetic predictors in 445 independent normo-glycemic individuals (the 500FG
96 cohort)²⁸(**Methods, Supplementary Figure 1**), and designed to capture sets of variants likely
97 to be enriched for association. On average, in LL-DEEP the identified genetic predictors
98 explained 13% (range 2%-30%) of variance in their respective microbiome features. The
99 average F-statistic, another measure of the strength of these genetic predictors, was 21.7
100 (range 15.3 - 25.5); an F-statistic >10 is considered sufficiently informative for MR
101 analyses²⁹.

102 We used the inverse-variance weighted (IVW) test to identify causal relationships between
103 the 245 microbiome features and the 17 traits of interest in a two-sample bidirectional MR
104 analysis using pairs of GWAS summary statistics (one from a microbiome feature and one
105 from a metabolic/anthropometric trait)²⁹. Based on principal component analysis (PCA) and
106 cluster analyses conducted on the microbiome and metabolic and anthropometric traits
107 (**Methods, Supplementary Figure 2**), we adopted a conservative multiple testing adjusted
108 threshold of $P < 1.3 \times 10^{-4}$ to declare a causal relationship significant. Because the presence

109 of horizontal pleiotropy (where a genetic predictor has independent effects on the diseases
110 through multiple traits) could bias the MR estimates, we investigated the robustness of
111 significant findings to pleiotropy by using three additional MR tests: the MR-PRESSO³⁰, the
112 weighted median test³¹, and the MR-Egger³². We formally examined the presence of
113 horizontal pleiotropy using the MR-PRESSO Global test³⁰ and the modified Rucker's Q'
114 test^{33,34}. Finally, we sought to validate these causal relationships in an independent cohort
115 (UK Biobank)³⁵ (**Figure 1**).

116 We observed a significant causal influence for one specific microbiome feature, a microbial
117 pathway involved in 4-aminobutanoate (GABA) degradation (MetaCyc designation PWY-
118 5022: 4-aminobutanoate degradation V) on increased insulin secretion, and specifically the
119 ratio of the areas under the curve for insulin and glucose, $AUC_{\text{insulin}}/AUC_{\text{glucose}}$, measured
120 during an oral glucose tolerance test (oGTT) (**Figure 2a**). Using nine genetic predictors
121 (variance explained = 16%; F-statistic = 21, **Supplementary Table 4**), we estimated that
122 each standard deviation (SD) increase in the abundance of PWY-5022 generated a 0.16
123 mU/mmol increase in $AUC_{\text{insulin}}/AUC_{\text{glucose}}$ ($P = 9.8 \times 10^{-5}$) (**Supplementary Table 5**,
124 **Supplementary Figure 3**). This causal relationship was robust when additional MR tests
125 were performed ($P_{\text{MR-PRESSO}} = 0.02$, $P_{\text{Weighted-Median}} = 0.02$ and $P_{\text{MR-EGGER}} = 0.02$), and there was
126 no evidence for horizontal pleiotropy ($P_{\text{MR-PRESSO}_{\text{global}}} = 0.18$ and $P_{\text{RuckerQ}'(\text{modified})} = 0.77$)
127 (**Supplementary Figure 4**). The reverse MR analysis (testing the relationship between
128 genetic predictors of $AUC_{\text{Insulin}}/AUC_{\text{glucose}}$ and PWY-5022 abundance) was not significant (P
129 > 0.1 , **Supplementary Table 6**). There was no evidence of causality with seven metabolic
130 and anthropometric traits (body-mass index (BMI), body fat %, waist-hip ratio (WHR),
131 visceral adipose tissue, abdominal subcutaneous adipose tissue, obesity and T2D) in a MR
132 analyses that used UK Biobank summary statistics (**Supplementary Table 7**); insulin
133 secretion phenotypes after oGTT were not available. We also found supportive evidence ($P <$

134 0.05) for a causal impact of this pathway on other insulin response parameters (**Figure 2b**).

135 Though other types of causal relationship are possible, these data are consistent with a model

136 whereby host genetic variation that influences gut microbiome composition so as to modulate

137 GABA degradation activity results in improvements in the capacity of the pancreatic islets to

138 secrete insulin in response to a physiological glucose challenge.

139 Butyrate and acetate are products of GABA degradation. In our taxonomic analyses, the

140 bacterial species most correlated with the abundance of PWY-5022 were *Eubacterium rectale*

141 and *Roseburia intestinalis* (Spearman $\rho = 0.52$ and 0.30 , respectively, **Figure 2c**), both well-

142 known butyrate-producing bacteria^{36,37}. Plasma butyrate levels were not measured in our

143 study; current assays are challenging to perform and provide unreliable estimates³⁸. Whilst

144 we consider the abundance of the PWY-5022 pathway to act as a proxy for butyrate

145 production in the gut, we were unable to directly link PWY-5022 abundance to the amount of

146 butyrate absorbed by the host. The abundance of PWY-5022 was poorly correlated with fecal

147 butyrate levels (Spearman $\rho = 0.1$), and we did not detect any causal relationships between

148 this SCFA and the 17 traits ($P > 0.05$), indicating that fecal butyrate is a poor proxy for

149 butyrate production and absorption.

150 These results point towards a causal role for gut-produced butyrate that is focused on the

151 dynamic insulin response to food ingestion, rather than the homeostatic mechanisms involved

152 in the maintenance of glucose metabolism in the fasted state. Independent clinical studies

153 support this hypothesis. For example, an intervention study evaluating the role of

154 *Bifidobacteria*-increasing prebiotics (fructo-oligosaccharides) in 35 healthy individuals

155 showed that prebiotics decrease levels of butyrate-producing bacteria and result in adverse

156 effect on glucose metabolism following an oGTT³⁹.

157 The PWY-5022 finding led us to consider the role of other SCFAs in metabolic and

158 anthropometric traits. In our cross-sectional analysis within LL-DEEP, we had detected

159 associations between fecal propionate levels and BMI (FDR < 0.1). Propionate is produced
160 by different bacteria than those producing butyrate⁴⁰, and its three genetic predictors
161 (variance explained = 6.3%, F-statistic = 21) were independent of those implicated in PWY-
162 5022 abundance (**Supplementary Table 4, 8**). In MR analyses for the 17 traits of interest, we
163 found that each SD increase in fecal propionate levels was causally associated with a 0.03 SD
164 increase in BMI ($P = 0.0068$) and an odd's ratio (OR) = 1.15 for T2D ($P = 0.004$)
165 (**Supplementary Table 9**), although these did not pass our significance threshold. No
166 associations were evident in the reverse MR analysis testing the effect of T2D and BMI on
167 fecal propionate levels ($P > 0.1$, **Supplementary Table 10**).

168 Of the two observed effects of fecal propionate, on BMI and T2D, the latter was more robust.
169 The causal relationship on increased T2D risk was robust when other MR tests were
170 performed ($P_{MR-PRESSO} = 0.03$, $P_{Weighted-Median} = 0.03$) and there was no evidence for pleiotropy
171 ($P_{MR-PRESSOglobal} = 0.75$, $P_{RuckerQ'(modified)} = 0.50$) (**Supplementary Figure 5**). By contrast, the
172 effect of propionate on increased BMI was not significant when using other MR tests and
173 there was also evidence for pleiotropy ($P_{MR-PRESSOglobal} = 2.0 \times 10^{-3}$, $P_{RuckerQ'(modified)} = 9.2 \times 10^{-4}$)
174 (**Supplementary Table 9, Supplementary Figure 6**). The pleiotropy in the BMI effect
175 could be accounted for by SNP rs7142308 (NC_000014.8:g.79482379A>G) (P_{MR-}
176 $PRESSO_{OutlierTest} = 0.01$), located within a BMI-associated locus²⁰ but independent of the lead
177 variant (rs7141420 (NC_000014.8:g.79899454C>T), $r^2 = 0.01$ with rs7142308 in 1000
178 Genomes Europeans).

179 Applying MR analyses to UK Biobank summary statistics, we replicated the relationship
180 between fecal propionate levels and increased risk of T2D ($P_{IVW} = 0.01$, $P_{MR-PRESSO} = 0.007$,
181 $P_{Weighted-Median} = 0.04$; $P_{IVWcombined} = 4 \times 10^{-5}$, **Figure 3**), and there was no evidence of
182 pleiotropy ($P_{MR-PRESSOglobal} = 0.97$, $P_{RuckerQ'(modified)} = 0.99$). The relationship between fecal

183 propionate and BMI was again not robust to pleiotropy, highlighting the need for caution in
184 interpreting this effect as causal (**Supplementary Table 11**).

185 Over 95% of gut-produced SCFAs are absorbed by the host⁴¹, such that increases in fecal
186 propionate levels could be the consequence of either increased production or reduced
187 absorption. The latter (which would link increased fecal propionate to reduced circulating
188 levels) would be more consistent with the preponderance of evidence that indicates that
189 SCFAs have a largely beneficial effect on energy balance and metabolic homeostasis^{4,10,12-14}.
190 As with plasma butyrate, plasma propionate levels were not measured in our cohorts. Further
191 studies are warranted to explore the mechanisms underlying this relationship between fecal
192 propionate levels and T2D.

193 In summary, these data are consistent with a causal role for gut-produced SCFAs, specifically
194 butyrate and propionate, with respect to energy balance and glucose homeostasis in man. We
195 have shown that a genetically-influenced shift in the gut microbiome towards increased
196 production of butyrate has beneficial effects on beta-cell function, though no impact on T2D
197 risk could be detected. We have also demonstrated that host genetic variation that results in
198 increased fecal propionate levels (reflecting some combination of increased production or
199 impaired absorption) has impact on T2D-risk.

200 Although the LL-DEEP cohort represents the largest population study on the genetics of
201 microbiome^{2,17,18}, it is still underpowered to capture the limited genetic component that has
202 been estimated for microbiome features¹⁹. The results from this and other microbiome
203 GWAS^{2,17,18} showed only limited direct overlap, highlighting the need for standardized
204 protocols for data analyses and larger sample size⁴². This will be crucial also in the context of
205 MR analyses, as expanded GWAS will deliver more robust genetic predictors⁴³. A better
206 understanding of the complex interplay between gut microbiome and host metabolism will
207 require expansion of current analyses and the ability to fold in measures of circulating

208 SCFAs. Nevertheless, this study demonstrates that microbiome GWAS provide a route to
209 causal inference that can guide and complement more direct experimental approaches, such
210 as those based around fecal transplantation and animal models. We envisage that with
211 expanded microbiome-genetic studies, for example the MiBioGen consortium⁴⁴, MR will
212 become a standard tool for systematically screening a large number of hypotheses generated
213 in current and future microbiome-wide association studies.

214

215 **URLs**

216 MAGIC: <https://www.magicinvestigators.org/>

217 GIANT: http://portals.broadinstitute.org/collaboration/giant/index.php/Main_Page

218 DIAGRAM: <http://www.diagram-consortium.org/>

219 UK Biobank: <http://www.ukbiobank.ac.uk/>

220 Human Functional Genomics Project: <http://www.humanfunctionalgenomics.org/>

221 Bracken: <https://github.com/jenniferlu717/Bracken>

222 MetaCyc metabolic pathway database: <http://www.metacyc.org/>

223 PLINK: www.cog-genomics.org/plink2

224 Michigan imputation server: <https://imputationserver.sph.umich.edu/>

225 R: <https://www.r-project.org/>

226 LD Score: <https://github.com/bulik/ldsc>

227 MR-PRESSO: <https://github.com/rondolab/MR-PRESSO>

228

229 **Acknowledgements**

230 We thank the participants and staff of the LL-DEEP cohort for their collaboration, the
231 UMCG Genomics Coordination center, the UG Center for Information Technology and their
232 sponsors BBMRI-NL & TarGet for storage and compute infrastructure. We are also grateful

233 to Marc Jan Bonder for help in formatting summary statistics, to Rinse K. Weersma and
234 Yang Li for discussions and to Kate Mc Intyre for editing the manuscript. Part of this work
235 was conducted using the UK Biobank resource under application number 9161.

236 This project was funded by: IN-CONTROL CVON grant CVON2012-03 to M.G.N., A.Z.,
237 L.J. and J.F.; Top Institute Food and Nutrition (TiFN, Wageningen, the Netherlands) grant
238 TiFN GH001 to C.W.; the Netherlands Organization for Scientific Research (NWO) grants
239 NWO-VENI 016.176.006 to M.O., NWO-VIDI 864.13.013 to J.F., and NWO-VIDI
240 016.Vidi.178.056 to A.Z; NWO Spinoza Prizes SPI 92-266 to C.W. and SPI 94-212 to
241 M.G.N.; the European Research Council (ERC)-Starting grant ERC #715772 to A.Z.; the
242 FP7/2007-2013/ERC Advanced Grant (agreement 2012-322698) to C.W.; the ERC
243 Consolidator Grant ERC#310372 to M.G.N.; Tripartite Immunometabolism consortium
244 (TriC) – Novo Nordisk Foundation Grant#NNF15CC0018486 to M.M.; and Wellcome grants
245 090532, 098381, 106130, and 203141 to M.M.. A.Z. also holds a Rosalind Franklin
246 Fellowship from the University of Groningen. M.M. is a Wellcome Senior Investigator, and a
247 National Institute of Health Research Senior Investigator. The funders had no role in study
248 design, data collection and analysis, decision to publish, or preparation of the manuscript.
249 The views expressed in this article are those of the author(s) and not necessarily those of the
250 NHS, the NIHR, or the Department of Health.

251 **Author Contributions**

252 S.S. performed statistical analyses in LifeLines and 500FG cohorts; N.vZ. and A.M.
253 performed statistical analyses in UK Biobank and DIAGRAM studies; A.K. and A.V.V.
254 processed raw microbiome data in Lifelines-DEEP and 500FG; U.V. and L.F. downloaded
255 and harmonized the summary statistics from GIANT, MAGIC and DIAGRAM consortia;
256 L.F., and C.W. provided LifeLines-DEEP data; Z.M., A.A.M.M., D.M.A.E.J. provided
257 critical input to manuscript revisions; M.O., L.J. and M.G.N. provided 500FG data; S.S.,

258 N.vZ. and M.M. wrote the manuscript, with critical input from J.F., A.Z. and C.W.; S.S.,
259 N.vZ., A.M., C.W. and M.M. designed the study. All authors read, revised and approved the
260 manuscript.

261 **Competing Interests statement**

262 M.M serves on advisory panels for Pfizer, NovoNordisk, Zoe Global; has received honoraria
263 from Pfizer, NovoNordisk and Eli Lilly; has stock options in Zoe Global; has received
264 research funding from Abbvie, Astra Zeneca, Boehringer Ingelheim, Eli Lilly, Janssen,
265 Merck, NovoNordisk, Pfizer, Roche, Sanofi Aventis, Servier, Takeda. All other authors
266 declare no competing financial interests.

267

268 **References**

- 269 1. Zhernakova, A. *et al.* Population-based metagenomics analysis reveals markers for gut
270 microbiome composition and diversity. *Science* **352**, 565-9 (2016).
- 271 2. Bonder, M.J. *et al.* The effect of host genetics on the gut microbiome. *Nat Genet* **48**, 1407-
272 1412 (2016).
- 273 3. Evans, D.M. & Davey Smith, G. Mendelian Randomization: New Applications in the Coming
274 Age of Hypothesis-Free Causality. *Annu Rev Genomics Hum Genet* **16**, 327-50 (2015).
- 275 4. Larsen, N. *et al.* Gut microbiota in human adults with type 2 diabetes differs from non-
276 diabetic adults. *PLoS One* **5**, e9085 (2010).
- 277 5. Karlsson, F.H. *et al.* Gut metagenome in European women with normal, impaired and
278 diabetic glucose control. *Nature* **498**, 99-103 (2013).
- 279 6. Ley, R.E. *et al.* Obesity alters gut microbial ecology. *Proc Natl Acad Sci U S A* **102**, 11070-5
280 (2005).
- 281 7. Kreznar, J.H. *et al.* Host Genotype and Gut Microbiome Modulate Insulin Secretion and Diet-
282 Induced Metabolic Phenotypes. *Cell Rep* **18**, 1739-1750 (2017).
- 283 8. Brunkwall, L. & Orho-Melander, M. The gut microbiome as a target for prevention and
284 treatment of hyperglycaemia in type 2 diabetes: from current human evidence to future
285 possibilities. *Diabetologia* **60**, 943-951 (2017).
- 286 9. Kootte, R.S. *et al.* Improvement of Insulin Sensitivity after Lean Donor Feces in Metabolic
287 Syndrome Is Driven by Baseline Intestinal Microbiota Composition. *Cell Metab* **26**, 611-619
288 e6 (2017).
- 289 10. Zhang, X. *et al.* Human gut microbiota changes reveal the progression of glucose intolerance.
290 *PLoS One* **8**, e71108 (2013).
- 291 11. Rios-Covian, D. *et al.* Intestinal Short Chain Fatty Acids and their Link with Diet and Human
292 Health. *Front Microbiol* **7**, 185 (2016).
- 293 12. Pingitore, A. *et al.* The diet-derived short chain fatty acid propionate improves beta-cell
294 function in humans and stimulates insulin secretion from human islets in vitro. *Diabetes*
295 *Obes Metab* **19**, 257-265 (2017).
- 296 13. Chambers, E.S. *et al.* Effects of targeted delivery of propionate to the human colon on
297 appetite regulation, body weight maintenance and adiposity in overweight adults. *Gut* **64**,
298 1744-54 (2015).
- 299 14. Zhao, L. *et al.* Gut bacteria selectively promoted by dietary fibers alleviate type 2 diabetes.
300 *Science* **359**, 1151-1156 (2018).
- 301 15. Peng, L., He, Z., Chen, W., Holzman, I.R. & Lin, J. Effects of butyrate on intestinal barrier
302 function in a Caco-2 cell monolayer model of intestinal barrier. *Pediatr Res* **61**, 37-41 (2007).
- 303 16. Schwartz, A. *et al.* Microbiota and SCFA in lean and overweight healthy subjects. *Obesity*
304 (*Silver Spring*) **18**, 190-5 (2010).
- 305 17. Turpin, W. *et al.* Association of host genome with intestinal microbial composition in a large
306 healthy cohort. *Nat Genet* **48**, 1413-1417 (2016).
- 307 18. Goodrich, J.K. *et al.* Genetic Determinants of the Gut Microbiome in UK Twins. *Cell Host*
308 *Microbe* **19**, 731-43 (2016).
- 309 19. Rothschild, D. *et al.* Environment dominates over host genetics in shaping human gut
310 microbiota. *Nature* **555**, 210-215 (2018).
- 311 20. Locke, A.E. *et al.* Genetic studies of body mass index yield new insights for obesity biology.
312 *Nature* **518**, 197-206 (2015).
- 313 21. Shungin, D. *et al.* New genetic loci link adipose and insulin biology to body fat distribution.
314 *Nature* **518**, 187-196 (2015).
- 315 22. Manning, A.K. *et al.* A genome-wide approach accounting for body mass index identifies
316 genetic variants influencing fasting glycemic traits and insulin resistance. *Nat Genet* **44**, 659-
317 69 (2012).

- 318 23. Strawbridge, R.J. *et al.* Genome-wide association identifies nine common variants associated
319 with fasting proinsulin levels and provides new insights into the pathophysiology of type 2
320 diabetes. *Diabetes* **60**, 2624-34 (2011).
- 321 24. Soranzo, N. *et al.* Common variants at 10 genomic loci influence hemoglobin A(1)(C) levels
322 via glycemc and nonglycemc pathways. *Diabetes* **59**, 3229-39 (2010).
- 323 25. Prokopenko, I. *et al.* A central role for GRB10 in regulation of islet function in man. *PLoS*
324 *Genet* **10**, e1004235 (2014).
- 325 26. Saxena, R. *et al.* Genetic variation in GIPR influences the glucose and insulin responses to an
326 oral glucose challenge. *Nat Genet* **42**, 142-8 (2010).
- 327 27. Scott, R.A. *et al.* An Expanded Genome-Wide Association Study of Type 2 Diabetes in
328 Europeans. *Diabetes* **66**, 2888-2902 (2017).
- 329 28. Li, Y. *et al.* A Functional Genomics Approach to Understand Variation in Cytokine Production
330 in Humans. *Cell* **167**, 1099-1110 e14 (2016).
- 331 29. Burgess, S., Butterworth, A. & Thompson, S.G. Mendelian randomization analysis with
332 multiple genetic variants using summarized data. *Genet Epidemiol* **37**, 658-65 (2013).
- 333 30. Verbanck, M., Chen, C.Y., Neale, B. & Do, R. Detection of widespread horizontal pleiotropy in
334 causal relationships inferred from Mendelian randomization between complex traits and
335 diseases. *Nat Genet* **50**, 693-698 (2018).
- 336 31. Bowden, J., Davey Smith, G., Haycock, P.C. & Burgess, S. Consistent Estimation in Mendelian
337 Randomization with Some Invalid Instruments Using a Weighted Median Estimator. *Genet*
338 *Epidemiol* **40**, 304-14 (2016).
- 339 32. Bowden, J., Davey Smith, G. & Burgess, S. Mendelian randomization with invalid
340 instruments: effect estimation and bias detection through Egger regression. *Int J Epidemiol*
341 **44**, 512-25 (2015).
- 342 33. Bowden, J. *et al.* Improving the accuracy of two-sample summary data Mendelian
343 randomization: moving beyond the NOME assumption. *Preprint at*
344 <https://www.biorxiv.org/content/early/2018/10/11/159442> (2018).
- 345 34. Rucker, G., Schwarzer, G., Carpenter, J.R., Binder, H. & Schumacher, M. Treatment-effect
346 estimates adjusted for small-study effects via a limit meta-analysis. *Biostatistics* **12**, 122-42
347 (2011).
- 348 35. Bycroft, C. *et al.* The UK Biobank resource with deep phenotyping and genomic data. *Nature*
349 **562**, 203-209 (2018).
- 350 36. Duncan, S.H., Hold, G.L., Barcenilla, A., Stewart, C.S. & Flint, H.J. Roseburia intestinalis sp.
351 nov., a novel saccharolytic, butyrate-producing bacterium from human faeces. *Int J Syst Evol*
352 *Microbiol* **52**, 1615-20 (2002).
- 353 37. Pryde, S.E., Duncan, S.H., Hold, G.L., Stewart, C.S. & Flint, H.J. The microbiology of butyrate
354 formation in the human colon. *FEMS Microbiol Lett* **217**, 133-9 (2002).
- 355 38. Jakobsdottir, G., Bjerregaard, J.H., Skovbjerg, H. & Nyman, M. Fasting serum concentration
356 of short-chain fatty acids in subjects with microscopic colitis and celiac disease: no difference
357 compared with controls, but between genders. *Scand J Gastroenterol* **48**, 696-701 (2013).
- 358 39. Liu, F. *et al.* Fructooligosaccharide (FOS) and Galactooligosaccharide (GOS) Increase
359 Bifidobacterium but Reduce Butyrate Producing Bacteria with Adverse Glycemc Metabolism
360 in healthy young population. *Sci Rep* **7**, 11789 (2017).
- 361 40. Louis, P. & Flint, H.J. Formation of propionate and butyrate by the human colonic
362 microbiota. *Environ Microbiol* **19**, 29-41 (2017).
- 363 41. den Besten, G. *et al.* The role of short-chain fatty acids in the interplay between diet, gut
364 microbiota, and host energy metabolism. *J Lipid Res* **54**, 2325-40 (2013).
- 365 42. Kurilshikov, A., Wijmenga, C., Fu, J. & Zhernakova, A. Host Genetics and Gut Microbiome:
366 Challenges and Perspectives. *Trends Immunol* **38**, 633-647 (2017).
- 367 43. Taylor, A.E. *et al.* Mendelian randomization in health research: using appropriate genetic
368 variants and avoiding biased estimates. *Econ Hum Biol* **13**, 99-106 (2014).

369 44. Wang, J. *et al.* Meta-analysis of human genome-microbiome association studies: the
370 MiBioGen consortium initiative. *Microbiome* **6**, 101 (2018).
371

372

373

374 **Figure Legends**

375 **Figure 1. Schematic representation of the study**

376 Figure 1 is a schematic representation of our study, highlighting for each step the research
377 question we want to answer, the analysis workflow, and the data used. We first aimed to
378 identify which microbiome feature (taxa, microbiome pathway or short-chain fatty acid
379 (SCFA)) correlated with metabolic traits in the LifeLines-DEEP (LL-DEEP) cohort (Step 1).
380 We then performed genome-wide association (GWA) analysis in LL-DEEP to identify
381 genetic predictors of those microbiome features (Step 2), and used the genetic predictors to
382 estimate causal relationships through bidirectional Mendelian Randomization analysis and
383 effect sizes for metabolic traits extracted from summary statistics of large GWA studies (Step
384 3). Finally, we validated our causality results using the UK Biobank (Step 4).

385

386 **Figure 2. Causal effect of butyrate-producing activity of the gut on glucose-stimulated**
387 **insulin response**

388 **a)** Schematic representation of the Mendelian Randomization analysis results: genetic
389 predisposition to higher abundance of butyrate-producing microbiome pathway PWY-5022
390 (4-aminobutanoate degradation V pathway) is associated with insulin response after glucose
391 challenge. The causal effect of PWY-5022 was also seen on other insulin response
392 parameters, and the forest plot in panel **(b)** represents the magnitude of the effect on each
393 parameter per one-standard-deviation increase in pathway abundance, as estimated in the
394 inverse-variance weighted Mendelian Randomization (MR) analysis. MR analysis was
395 carried out using up to nine genetic predictors and their effect size from LL-DEEP (952
396 samples) and MAGIC summary statistics (trait specific sample sizes are:
397 $AUC_{\text{insulin}}/AUC_{\text{glucose}} = 4213$; insulin at 30 min = 4,409; $AUC_{\text{insulin}} = 4,324$; correct insulin
398 response = 4,789; insulin increase at 30 min = 4,447; Disposition index = 5,130) (**Methods,**

399 **Supplementary Table 4 and 5**). Corresponding two-sided *P*-values are given in the annexed
400 table. **(c)** Correlation plots with PWY-5022 abundance and the bacteria correlating the most
401 with it in 950 LL-DEEP samples (subset of the 952 normo-glycemic samples for which
402 presence of those bacteria was detected). The Spearman correlation coefficient ρ is given in
403 blue in each panel.

404

405 **Figure 3. Causal effect of fecal propionate on type 2 diabetes (T2D)**

406 **a)** Schematic representation of the Mendelian Randomization analysis results: genetic
407 predisposition to higher fecal propionate levels is associated with increased risk of T2D. **b)** A
408 forest plot depicts the magnitude of the causal effect on T2D per each one-standard-deviation
409 increase in fecal butyrate levels, as estimated by the inverse-variance weighted Mendelian
410 Randomization (MR) analysis. MR analysis was carried out using the three genetic predictors
411 derived in LifeLines-DEEP (LL-DEEP) and their effects in the discovery data set
412 (DIAGRAM; 26,676 T2D cases and 132,532 controls) and in the replication cohort (UK
413 Biobank; 19,119 T2D cases and 423,698 controls). The effect derived combining the two
414 causal effects (from discovery and replication) with an inverse-variance weighted meta-
415 analysis approach is also given. Corresponding two-sided *P*-values are listed in the annexed
416 table. OR, odd's ratio.

417

418 **Online Methods**

419

420 **Study samples**

421 The discovery cohort of this study is Lifelines-DEEP (LL-DEEP), a population-based cohort of
422 1,539 individuals from Northern Netherlands (age range 18–84 years) that is a subset of the
423 largest Lifelines biobank (N = 167,000). For all LL-DEEP volunteers, an extensive dataset of
424 measured and self-reported phenotypic information has been collected, as well as blood
425 and stool specimens, all as described previously^{45,46}. Measurement of SCFAs in stool was
426 carried out by gas chromatography-mass spectrometry following the method of García-
427 Villalba et al⁴⁷.

428 To identify the appropriate threshold for the selection of genetic predictors of microbiome
429 features we used the 500 Functional Genomics (500FG) cohort²⁸, an independent cohort of
430 534 healthy individuals from the Netherlands (age-range 18-75 years). Protocols for stool
431 collection and metagenomic sequencing were similar to those used in LL-DEEP, as previously
432 described⁴⁸.

433 All participants from both studies signed an informed consent form. The LL-DEEP study was
434 approved by the institutional ethics review boards of the UMCG (ClinicalTrials.gov
435 NCT00775060). The 500FG study was approved by the Ethical Committee of Radboud
436 University Nijmegen (NL42561.091.12, 2012/550).

437 To replicate our findings we used genotype and phenotype data from the UK Biobank, a
438 study of 500,000 subjects from the United Kingdom aged 45-65 years of age³⁵. Each
439 participant provided a blood sample for DNA extraction and completed a detailed

440 questionnaire providing baseline data. Individuals are also linked to electronic medical
441 records on a number of traits including BMI and T2D.

442

443 **Data generation and pre-processing**

444 ***Genotyping***

445 Genotype data was available for 1,268 LL-DEEP volunteers, as previously described^{2,45}. In
446 brief, genotyping was carried out using two Illumina arrays, HumanCytoSNP-12 BeadChip
447 and ImmunoChip. After standard per-sample and per-SNP quality control filters, data from
448 the two arrays were merged and additional markers were imputed using the HRC reference
449 panel v1.1⁴⁹ on the Michigan server (see URLs). For our analyses, we focused on 15,001,957
450 variants with imputation accuracy RSQR > 0.3. In the 500FG cohort, 516 samples were
451 genotyped using the Illumina Human OmniExpress Exome-8 v1.0 SNP chip and, after
452 standard quality controls checks²⁸, were imputed using the same procedure and reference
453 panel used with LL-DEEP. The UK Biobank samples were genotyped using the Affymetrix UK
454 BiLEVE Axiom array on an initial 50,000 participants. The remaining 450,000 participants
455 were genotyped using the Affymetrix UK Biobank Axiom[®] array³⁵. Quality control on
456 samples and genotypes were performed centrally and subsequent imputation was
457 performed using the HRC reference panel at the Wellcome Centre Human Genetics.

458

459 ***Metagenomic sequencing***

460 Metagenomic sequencing of the gut microbiome was performed using the Illumina HiSeq
461 platform on 1,179 LL-DEEP samples. After applying per-sample and per-read quality filters²,
462 the profile of microbial composition was determined using Bracken pipeline (see URLs). In

463 total, 903 taxonomies were identified and normalized using a log transformation;
464 normalized non-zero values were then adjusted for age, sex and read depth using linear
465 regression.

466 Functional profiling was performed using HUMAnN2 (v 0.4.0), which maps reads to a
467 customized database of functionally annotated pan-genomes⁵⁰. This analysis identified 742
468 pathways from the MetaCyc metabolic pathway database⁵¹. Similar to the taxonomy data,
469 we normalized pathway abundances using log transformation and corrected the normalized
470 nonzero values for age, sex and read depth. We considered only non-zero values for
471 analyses, and therefore restricted analyses to microbiome features (taxonomies and
472 pathways) that had non-zero values in less than 50% of the samples and retained only one
473 of pairs of pathways or bacteria showing > 0.99 Spearman correlation. This filtering resulted
474 in a final set of 796 features (273 taxa and 523 pathways) that were used for analyses.

475 We further confined all statistical analyses to normo-glycemic samples with good quality
476 genetic and microbiome data. Normo-glycemic status was assigned to samples from
477 individuals not reported to have diabetes or to be taking oral anti-diabetes medications and
478 who had fasting glucose levels < 7 mmol/L. We also removed individuals who were taking
479 antibiotics at the time of the stool collection. This filtering resulted in a final set of 952
480 samples available for analyses. In the 500FG cohort, we used the same filters and selected
481 445 normo-glycemic samples with both genetic and microbiome data for analyses.

482 ***Genome-wide association scans of anthropometric and glycemic traits***

483 We downloaded full GWAS summary statistics from 9 studies that represented 17 GWAS for
484 different anthropometric and glycemic traits. These traits were BMI and waist-hip-ratio
485 (WHR), fasting glucose, insulin and pro-insulin, 2hr glucose, HOMA-derived measurements
486 of insulin resistance (HOMA-IR) and sensitivity (HOMA-B)), glycated hemoglobin (HbA_{1c}),

487 T2D, and 7 insulin response parameters measured during an oral glucose tolerance test
488 (oGTT) (**Supplementary Table 1** and URLs). SNP names and genomic positions were
489 aligned to the genomic build GRCh37/hg19.

490

491 **Statistical Analysis**

492 ***Correlation of short chain fatty acids and microbiome features with anthropometric and*** 493 ***glycemic traits***

494 We correlated 5 short chain fatty acids (Acetate, Butyrate, Propionate, Calproate and
495 Valerate) and 796 other microbiome features (taxa or pathways) with measured
496 anthropometric (BMI and WHR) and glycemic traits (fasting glucose, insulin, HbA_{1c},
497 HOMA-IR and HOMA-B) in the LL-DEEP cohort. Anthropometric and glycemic traits were
498 adjusted for age, sex, and BMI (except for BMI phenotype). We used the non-parametric
499 Spearman correlation test (*cor.test(method="Spearman")*) function in R (v3.3)) and
500 considered results significant when the multiple-testing-adjusted two-sided *P*-value was <
501 0.1. The multiple-testing-adjusted *P*-value, FDR *P*, was calculated using the Benjamini-
502 Hochberg procedure in the *p.adjust()* function in R (v3.3) (see URLs).

503

504 ***Genome-wide association analyses of short-chain fatty acids and microbiome features***

505 For each microbiome feature and short-chain fatty acid, we performed a genome-wide
506 association scan in LL-DEEP samples by re-processing data from our previous study in a
507 different manner². In particular: a) we re-mapped metagenomic reads to a more recent
508 database, b) we restricted analyses to only normo-glycemic samples and those who were no
509 under antibiotics, and c) we performed genetic analyses using a linear mixed model that
510 accounts for population structure instead of the Spearman correlation method. In particular
511 for genetic analyses, we used EPACTS (v3.2.6)⁵², a software program that performs a linear

512 mixed model adjusted with a genomic-based kinship matrix that is calculated using all
513 quality-checked genotyped autosomal SNPs with minor allele frequency > 1%. The
514 advantage of this model is that the kinship matrix encodes a wide range of sample structures,
515 including both cryptic relatedness and population stratification; this produces more robust
516 results than standard linear regression. All traits were inverse quantile normalized before
517 genetic analysis. Specifically for SFCAs, age, sex, Chromogranin A, stool type according to
518 Bristol scale, and BMI were added as covariates.

519 The variance explained (adjusted R squared) and the F-statistic for each microbiome feature
520 were extracted from a linear model that fitted all the selected genetic predictors on the
521 normalized, covariates-adjusted microbiome feature.

522

523 ***Mendelian Randomization analyses with 17 GWAS traits***

524 The Mendelian Randomization procedure consists of two steps: i) identification of proper
525 instrumental variables or genetic predictors, e.g. variants independently associated with the
526 exposure factor, and ii) calculation of causal estimates. For each GWAS summary statistic,
527 we first selected independent SNPs using the clumping procedure in *PLINK* v1.9 (see URLs)
528 and setting a linkage disequilibrium threshold of $r^2 < 0.1$ in a 500-Kb window. Linkage
529 disequilibrium was calculated using the LL-DEEP cohort when running the clumping
530 procedure on the GWAS of microbiome features and short chain fatty acids, whereas for
531 GWAS of anthropometric and glyceemic traits we used the linkage disequilibrium estimates
532 from the 1000 Genomes phase 3 European samples.

533 Furthermore, since the majority of the downloaded GWAS were based on the HapMap2
534 genetic map, for each independently associated variant, we identified the best HapMap2
535 proxy ($r^2 > 0.8$) or discarded that variant if no proxy was available.

536 Finally, we selected only variants that showed association at $P < 1 \times 10^{-5}$. We identified this
537 as the optimal P -value threshold to use for selection of genetic predictors associated with
538 microbiome features because this threshold led to a larger variance explained, on average, of
539 the same microbiome features in the 500FG cohort (**Supplementary Figure 1**). For
540 consistency, we used the same threshold and procedure for selecting genetic predictors from
541 the downloaded GWAS on anthropometric and glyceemic traits.

542 To calculate causal estimates, we used the inverse-variance weighted (IVW) method³² as a
543 two-sample MR analysis of summary association statistics of the exposure and the outcome.
544 Specifically, we estimated the causal effect in a fixed-effect meta-analysis framework, i.e. as
545 a sum of single-SNP causal effects (derived as a ratio of the SNP-effect on the outcome by
546 the SNP-effect on the exposure) weighted by the inverse of their variance (derived as a
547 squared ratio of the SNP-standard deviation on the outcome on SNP-effect on the
548 exposure). The P -value was calculated as $P = 2 * (1 - \Phi(Z))$, where $\Phi(Z)$ is the standard normal
549 cumulative distribution function and Z is ratio of the combined (using inverse variance
550 weights) causal effect and its standard error. Of note, the causal estimate is equivalent to
551 that obtained as a weighted linear regression of the outcome SNP-effects on the exposure
552 SNP-effects with a fixed intercept of 0 and with the inverse of the variance of the effect sizes
553 on the outcome as weights. For analyses, we set the effect allele of the genetic predictors to
554 be the allele with the positive direction. We also calculated causal estimates using additional
555 MR methods: MR-PRESSO³⁰, which removes pleiotropy by identifying and discarding
556 influential outlier predictors from the IVW test and uses a t-test to calculate P -values; the
557 weighted-median test³¹, which uses a statistical estimator that is robust to the presence of
558 pleiotropy in a subset ($< 50\%$) of the predictors; and the MR-Egger³², which adjusts for
559 average horizontal pleiotropy and assumes that $> 50\%$ of the predictors have pleiotropy.

560 Furthermore, we specifically evaluated presence of pleiotropy using MR-PRESSO Global test
561 ³⁰ and the modified Rücker's Q' test³³.

562

563 ***Calculation of significance threshold***

564 To define our significance threshold for the IVW-based MR analyses, we first run a principal
565 component analysis of the 245 microbiome features, and observed that the total variability
566 could be explained by the first 57 principal component axes. To derive the number of
567 independent anthropometric and metabolic traits out of the 17 of interest, we used pairwise
568 genetic correlation calculated using LDscore regression (LDscore v1.0.0). Variants were
569 restricted to those from HapMap3 and pre-computed LD Scores estimated in subjects of
570 European descent were used as recommended by the authors⁵³. Traits were hierarchically
571 clustered based on genetic correlation values ρ_g , with dissimilarity metric $(1-\rho_g)/2$
572 (**Supplementary Figure 2**). The number of resulting clusters was used to define the number
573 of independent traits. Genetic correlation could not be calculated with four insulin secretion
574 traits so we counted these as fully independent traits. We set our multiple testing significance
575 threshold at 1.3×10^{-4} ($0.05/(57*7)$).

576

577 ***Mendelian randomization analyses in UK Biobank***

578 We first calculated association of the 12 genetic predictors (9 for PWY-5022 and 3 for fecal
579 propionate) with 7 metabolic and anthropometric traits (BMI, body Fat %, WHR, visceral
580 adipose tissue (VAT), subcutaneous adipose tissue (SAT), obesity and T2D) using a linear
581 mixed model as implemented in BOLT-LMM (v2.3.2)⁵⁴. T2D status was defined according
582 to the definition used by Eastwood et al.⁵⁵; BMI was defined according to that used by the
583 GIANT consortium²⁰ and obesity was defined by ICD code 278. Analyses were restricted to
584 442,817 unrelated individuals of European descent and were adjusted for age, sex,

585 genotyping array and 6 genetic principal components; WHR was also adjusted for BMI. We
586 then used the summary statistics at these 12 variants to estimate causal relationships and
587 investigate presence of pleiotropy by applying the same statistical tests that were used with
588 the GWAS summary statistics and described in the previous paragraph.

589

590 **Reporting Summary**

591 Further information on research design is available in the Life Sciences Reporting Summary
592 linked to this article.

593

594 **Data availability**

595 The LifeLines-DEEP metagenomics sequencing data are available at the European Genome-
596 phenome Archive (EGA), with access code EGAS00001001704. Genotype and phenotype
597 data can be requested from the Lifelines Biobank
598 <https://www.lifelines.nl/researcher/biobank-lifelines/application-process>.

599 Summary statistics for metabolic traits were downloaded from MAGIC, GIANT and
600 DIAGRAM websites (see URLs).

601

602

603

604

605 **Methods-Only References**

- 606 45. Tigchelaar, E.F. *et al.* Cohort profile: LifeLines DEEP, a prospective, general population cohort
607 study in the northern Netherlands: study design and baseline characteristics. *BMJ Open* **5**,
608 e006772 (2015).
- 609 46. Li, N. *et al.* Pleiotropic effects of lipid genes on plasma glucose, HbA1c, and HOMA-IR levels.
610 *Diabetes* **63**, 3149-58 (2014).
- 611 47. Garcia-Villalba, R. *et al.* Alternative method for gas chromatography-mass spectrometry
612 analysis of short-chain fatty acids in faecal samples. *J Sep Sci* **35**, 1906-13 (2012).
- 613 48. Schirmer, M. *et al.* Linking the Human Gut Microbiome to Inflammatory Cytokine Production
614 Capacity. *Cell* **167**, 1125-1136 e8 (2016).
- 615 49. McCarthy, S. *et al.* A reference panel of 64,976 haplotypes for genotype imputation. *Nat*
616 *Genet* **48**, 1279-83 (2016).
- 617 50. Franzosa, E.A. *et al.* Species-level functional profiling of metagenomes and
618 metatranscriptomes. *Nat Methods* **15**, 962-968 (2018).
- 619 51. Vatanen, T. *et al.* Variation in Microbiome LPS Immunogenicity Contributes to Autoimmunity
620 in Humans. *Cell* **165**, 842-53 (2016).
- 621 52. Kang, H.M. *et al.* Variance component model to account for sample structure in genome-
622 wide association studies. *Nat Genet* **42**, 348-54 (2010).
- 623 53. Bulik-Sullivan, B.K. *et al.* LD Score regression distinguishes confounding from polygenicity in
624 genome-wide association studies. *Nat Genet* **47**, 291-5 (2015).
- 625 54. Loh, P.R. *et al.* Efficient Bayesian mixed-model analysis increases association power in large
626 cohorts. *Nat Genet* **47**, 284-90 (2015).
- 627 55. Eastwood, S.V. *et al.* Algorithms for the Capture and Adjudication of Prevalent and Incident
628 Diabetes in UK Biobank. *PLoS One* **11**, e0162388 (2016).

629

630 Editorial summary:

631 Mendelian Randomization analyses using genotyping data, gut metagenomic sequence and fecal
632 short chain fatty acid levels from 952 individuals combined with GWAS data show evidence of a
633 causal effect of the gut microbiome on metabolic traits.

634

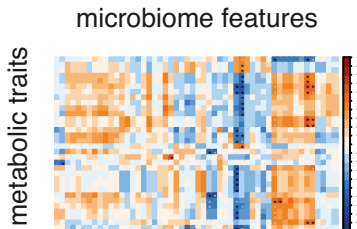
635

1. Which microbiome features correlate with metabolic traits?

LL-DEEP cohort

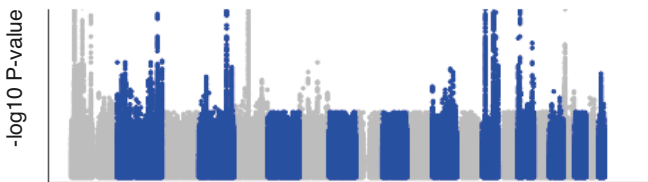


952 samples with:
metabolic traits
gut metagenomics data
genetic data



2. What are the genetic predictors of those individual microbiome features?

GWAS for microbiome feature X

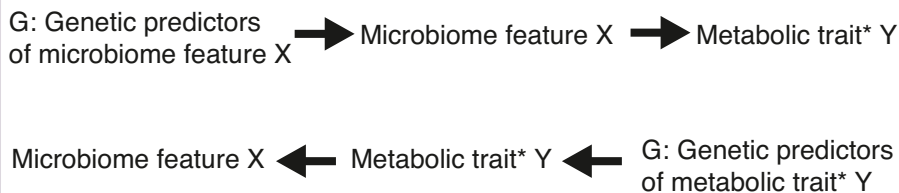


3. Do changes in microbiome features causally affect metabolic traits, or vice versa?

* GWAS summary stats from MAGIC, GIANT, DIAGRAM

SNP	Allele	Effect
rs2207139	G	0.04
rs2817419	A	0.07
rs1319136	A	-0.51
....

Bi-directional Mendelian Randomization



4. Can we replicate causal relationships?

UK Biobank



500,000 samples with:
genetic data
metabolic traits

Mendelian Randomization

